Measurements of magnetic moments in ^{150}Sm

T. Vass, A. W. Mountford, G. Kumbartzki, and N. Benczer-Koller
Department of Physics and Astronomy, Rutgers University, New Brunswick, New Jersey 08903

R. Tanczyn
Department of Physical Science, Kutztown University, Kutztown, Pennsylvania 19530

(Received 29 June 1993)

The magnetic moments of the 4_1^+ and 6_1^+ states in ^{150}Sm relative to that of the 2_1^+ state have been measured by the transient field technique. The resulting g-factor ratios are $g(4_1^+)/g(2_1^+) = 1.60(12)$ and $g(6_1^+)/g(2_1^+) = 1.14(34)$. The $g(4_1^+)/g(2_1^+)$ ratio is larger than expected for a collective band. To confirm this result a variety of measurements were conducted with both ^{32}S and ^{58}Ni beams at energies ranging from 80 to 230 MeV incident on targets with both iron and gadolinium ferromagnetic layers.

PACS number(s): 21.10.Ky, 27.70.+q

I. INTRODUCTION

The magnetic moments of nuclei have traditionally made an important contribution to nuclear structure research because they provide a sensitive test of differing theoretical descriptions.

Medium weight nuclei far-from-closed shells have been best described by collective models. The g factors of the low-lying states of such nuclei are expected to be equal to Z/A, corresponding to the fact that protons and neutrons in a nucleus are assumed to participate equally in the collective motion [1]. Many g factors of the first 2^+ states of even-even nuclei in medium weight nuclei and in the region $84 \leq N \leq 92$ and $Z = 60, 62$ have been measured [2,3]. Deviations from the Z/A prediction were attributed to the effect of pairing, single-particle contributions or subshell closure at $Z = 64$ and were successfully described within the framework of the interacting boson approximation (IBA) [4].

Magnetic moments of higher spin states along the yrast band have also been measured in rotational rare-earth nuclei with $64 < Z < 70$ and $N > 90$ [5,6]. In general, the moments remain fairly constant at low spin, *decrease* at higher spin, and have been noted to *increase* at yet higher spins. These observations were first explained in the framework of the cranked shell model approach as being due to rotational alignment of $i_{13/2}$ neutrons followed by alignment of protons [7]. Self-consistent cranked Hartree-Fock-Bogoliubov calculations [8] have also been very successful in describing the trends observed in several nuclei.

For transitional rare-earth nuclei with neutron number close to 90, a simplified model calculation was performed in the Nilsson-Strutinsky plus BCS approach by calculating the spin dependence of the deformation and pairing gaps [9]. These calculations predict a gradual *increase* of g factors with angular momentum increasing up to $10\hbar$ for ^{160}Yb, and a more dramatic rise for ^{154}Dy; similar effects are expected for ^{152}Gd and ^{150}Sm. The magnetic moments of the yrast states in ^{154}Dy have been recently measured [10]. Whereas the decrease in the moments of states above spin 20 has indeed been observed, the predicted rise of the magnetic moments of the low-lying states was not confirmed. Thus it becomes interesting to further test the model in ^{150}Sm and ^{152}Gd.

Most magnetic moments of short-lived states are measured through the transient field technique [11,12] applied to nuclear states populated either by Coulomb excitation or by (HI,xn) reactions. The time history of deexciting nuclei produced in (HI,xn) reactions is not always well established, particularly for low-spin states, setting limitations on the measurement of the magnetic interaction between the excited nucleus and the host ferromagnet. However, if the low-lying states can be reached by Coulomb excitation, their moments can be determined with higher reliability.

The magnetic moment of the 2_1^+ state in ^{150}Sm, $g = 0.385(27)$, has been measured by different techniques, such as recoil implantation into gas, ion-implantation perturbed angular correlation, and the transient field [13,14,2,3]. There is, however, only one transient field measurement of the magnetic moments of the 4_1^+ and 6_1^+ states which yields ratios $g(4_1^+)/g(2_1^+)$=0.87(10) and $g(6_1^+)/g(2_1^+)$=0.94(19), close to unity [15].

In the present study, the magnetic moments of the 2_1^+, 4_1^+, and 6_1^+ states in the ^{150}Sm nucleus were also measured by the transient field technique [16]. A variety of experimental conditions were used, and a new analysis procedure was developed to reduce possible systematic errors.

II. EXPERIMENTAL PROCEDURES

The transient field technique has been presented in several earlier publications [11,12] and only details pertain-

ing to the current experiment will be given here.

The experiments were performed at the A. W. Wright Nuclear Structure Laboratory at Yale University. Heavy-ion beams of ^{58}Ni or ^{32}S with energies ranging from 80 to 230 MeV were used to Coulomb-excite either the 2_1^+, or the 2_1^+ and 4_1^+, or the 2_1^+, 4_1^+, and 6_1^+ states of ^{150}Sm. Other states were only weakly excited. Their contributions were nevertheless taken into account even though they had only a minor effect on the results. The level scheme and properties of the low-lying states in ^{150}Sm are shown in Fig. 1. The lifetime of the 6_1^+ state is not known. The line shape of the $6_1^+ \rightarrow 4_1^+$ transition in the measurement is consistent with a lifetime of approximately 2 ps.

The beam-target configurations as well as the composition of the individual targets of seven different runs are summarized in Tables I and II. Targets consisted of enriched ^{150}Sm (99.23%) evaporated onto natural gadolinium or iron foils rolled to a thickness determined by the desired exit velocity of the recoil ions $v \geq 2v_0$, where v_0 is the Bohr velocity. The gadolinium foils were annealed under vacuum (10^{-6} Torr) by resistance heating, while the iron foils were annealed at 800 °C for 1 h in a hydrogen atmosphere to insure good magnetic properties. Layers of copper or silver thick enough to stop the recoiling ^{150}Sm ions were evaporated on the back side of the ferromagnetic layer. The magnetization of each target was measured with a 5% accuracy before and after each run as a function of temperature and external polarizing field by a double coil induction magnetometer [17].

An external magnetic field large enough to fully saturate the ferromagnetic foils, 0.043 T for iron and 0.09 T for gadolinium, was applied to the targets. The field direction was reversed periodically at time intervals of about 4 min. The targets with gadolinium as the ferromagnet were mounted at the tip of a closed-cycle Displex refrigerator and were kept at a temperature ranging between 40 K and 60 K in-beam. The dependence of the gadolinium target magnetization on temperature and external field is displayed in Fig. 2.

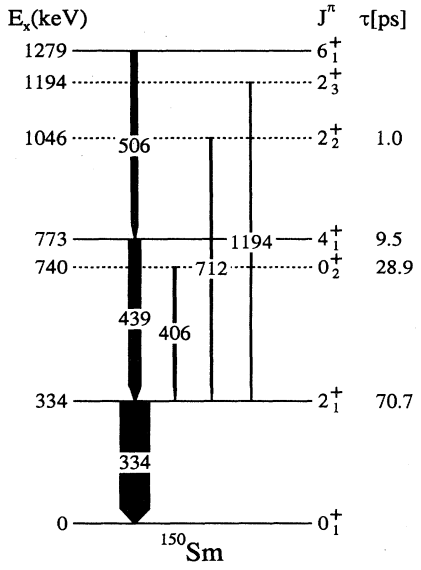

FIG. 1. Low-lying states in ^{150}Sm observed in the ^{150}Sm(^{58}Ni,^{58}Ni γ)^{150}Sm reaction at 230 MeV.

TABLE I. Summary of beam/detector/target configurations used in different runs.

Run	Beam	Beam energy (MeV)	Detectors	Ferromagnet	Stopper
I	^{32}S	80	NaI(Tl)	Fe	Cu
II	^{58}Ni	230	NaI(Tl)	Fe	Ag
III	^{58}Ni	230	NaI(Tl)	Gd	Cu
IV	^{58}Ni	230	Ge	Gd	Cu
V	^{58}Ni	180	Ge	Gd	Cu
VI	^{58}Ni	120	Ge	Gd	Cu
VII	^{32}S	115	NaI(Tl)	Fe	Cu
Ref. [15]	^{58}Ni	220	Ge	Fe	Pb

The deexcitation γ rays from ^{150}Sm were detected in coincidence with backscattered beam ions. Four Ge detectors (approximately 20% efficiency) and when appropriate, four 17.6 cm by 17.6 cm NaI(Tl) detectors were operated in coincidence with an annular silicon surface barrier detector subtending a solid angle of 165°–175°. For the precession measurement, the four Ge or NaI(Tl) γ-ray detectors were placed at angles of ($\pm 67°, \pm 113°$), or ($\pm 63°, \pm 117°$), respectively, where the logarithmic slope $S = (1/W)(dW/d\theta)$ of the γ-ray angular correlation $W(\theta)$ is large for $E2$ transitions.

The energies of coincident γ rays and particles together with their relative times were recorded in event mode and stored on magnetic tape using the Oak Ridge Data Acquisition System. With appropriate cuts in the particle [Fig. 3(a)] and time spectra, final γ-ray spectra [Fig. 3(b)] were produced, and peak intensities of the ^{150}Sm transitions were determined.

III. DATA ANALYSIS AND RESULTS

A. Angular distribution analysis

Under the experimental conditions used for the present experiment, any one state of interest is populated separately by multiple Coulomb excitation and by radiative decay of higher states. The alignment produced by these two mechanisms is different and induces a different angular distribution for the decay γ rays. It is not possible to physically separate the states populated by Coulomb excitation from the ones resulting from the γ decay of higher states from the γ-ray spectra. Furthermore, the Coulomb excitation probability of each individual state is not known *a priori* for a nonrotational nucleus like ^{150}Sm which lies between the almost spherical ^{148}Sm and the well-deformed ^{154}Sm. Therefore, simultaneous fits to the angular correlation of any of the γ rays in the $6_1^+ \rightarrow 4_1^+ \rightarrow 2_1^+ \rightarrow 0_1^+$ or $4_1^+ \rightarrow 2_1^+ \rightarrow 0_1^+$ cascades that are observed in the particular run being analyzed, were carried out with the relative Coulomb excitation probabilities as free parameters.

TABLE II. Summary of target configuration and kinematics of the recoiling ion. l is the thickness of the ^{150}Sm target isotope. L is the thickness of the ferromagnetic foil. M is the magnetization of the ferromagnetic layer measured before and after each run at the given external magnetic field H_{ext}. $\langle E\rangle_{in}$ and $\langle E\rangle_{out}$ are the average energies of the ^{150}Sm recoils. $\langle v/v_0\rangle$ is the average ion velocity in units of the Bohr velocity $v_0 = e^2/\hbar$ and t_m is the transit time through the ferromagnetic foil.

Run	l (mg/cm^2)	L (mg/cm^2)	H_{ext} (T)	M (T)	$\langle E\rangle_{in}$ (MeV)	$\langle E\rangle_{out}$ (MeV)	$\langle \frac{v}{v_0}\rangle_{in}$	$\langle \frac{v}{v_0}\rangle_{out}$	t_m (ps)
I	0.76	1.77	0.043	0.1551	40.1	12.4	3.3	1.8	0.42
II	1.43	4.30	0.043	0.1623	157.4	25.5	6.5	2.6	0.59
III	0.93	7.08	0.090	0.1701	166.7	36.7	6.7	3.1	0.88
IV	0.93	7.08	0.090	0.1701	166.7	36.7	6.7	3.1	0.88
V	0.93	7.08	0.090	0.1701	127.8	22.7	5.9	2.5	1.07
VI	0.93	7.08	0.090	0.1701	82.0	9.4	4.7	1.6	1.47
VII	0.76	1.77	0.043	0.1551	59.1	22.6	4.0	2.5	0.33
Ref. [15][a]	3.0(1)	4.1(1)	0.050	-	122.0	16.3	5.7	2.1	0.67

[a]The target used in Ref. [15] was a complex target containing a 0.10(2) mg/cm^2 indium layer between the ^{150}Sm and the ferromagnet.

The γ-ray radiations involved in the decay of these states are all "stretched $E2$" transitions. Thus, the angular distributions of all the γ rays in a particular cascade depopulating any one of the initial states are the same.

The measured γ-ray angular distributions for the individual cascade transitions can be fitted simultaneously to the theoretical expression

$$W^n(\theta; I_n \rightarrow I_{n-1}) = A \sum_{i=n}^{n_{max}} P_i W(\theta; I_i \rightarrow I_{i-1}), \quad n = 1, 2, ..., n_{max}, \quad (1)$$

where A is a normalization factor depending on the beam current, measurement time, detector efficiency, and geometry, P_i are the direct excitation probabilities of the individual excited states, n denotes the excited level, n_{max} represents the highest excited state, and $n = 0$ is the ground state. $W(\theta; I_i \rightarrow I_{i-1})$ are the theoretical angu-

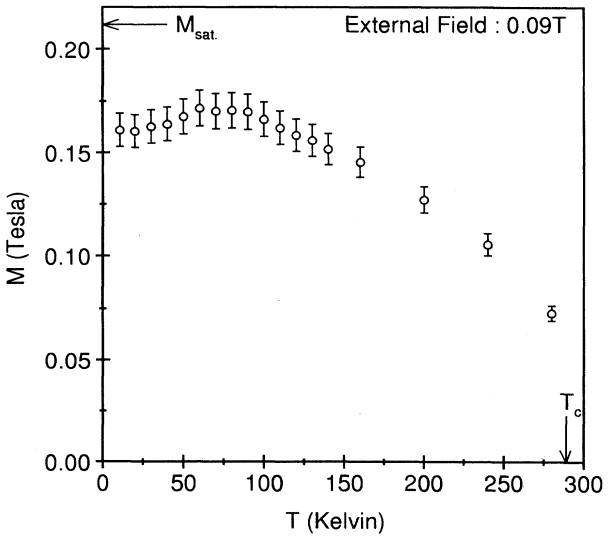

FIG. 2. Temperature dependence of the gadolinium target magnetization used in run III–VI precession measurements at an external polarizing field of 0.09 T. The error bars represent a 5% uncertainty in the magnetization measurements. $M_{sat.}$=0.2115 T or 268.4 emu/g is the saturation magnetization for gadolinium at 0 K. T_C=295 K is the Curie temperature for gadolinium.

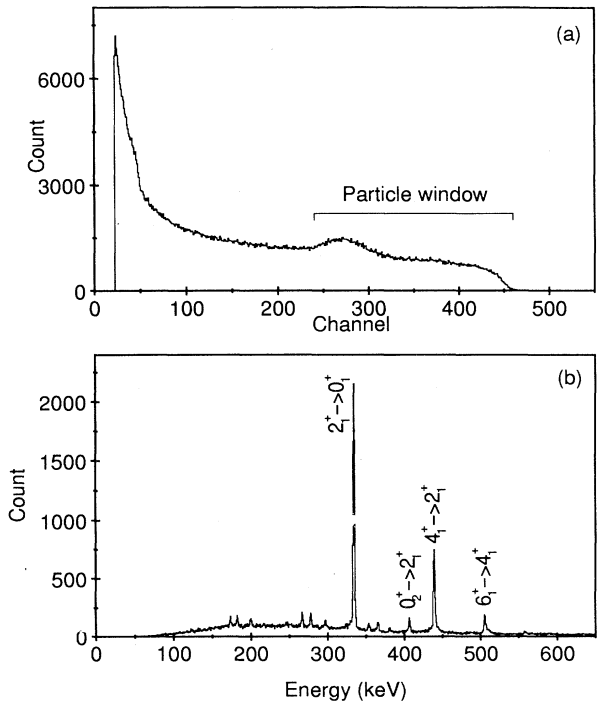

FIG. 3. (a) Typical coincidence particle spectrum of 230 MeV ^{58}Ni ions backscattered from ^{150}Sm, (b) corresponding γ-ray spectrum in coincidence with ^{58}Ni ions with energy in the indicated particle window (a). The unlabeled γ-ray triplets in the 350, 280, and 185 keV regions correspond, respectively, to the $8_1^+ \rightarrow 6_1^+$, $6_1^+ \rightarrow 4_1^+$, and $4_1^+ \rightarrow 2_1^+$ transitions in ^{156,158,160}Gd.

lar distributions of pure $I_i \rightarrow I_{i-1}$ transitions. This expression can be modified to take into account side feeding from other cascades. The ground- and higher state excitation probabilities, $P_{\text{g.s.}}$ and P_i, are normalized such that

$$1 = P_{\text{g.s.}} + \sum_{i=1}^{n_{\max}} P_i. \quad (2)$$

The theoretical angular distributions of the pure $E2$ $I_i \rightarrow I_{i-1}$ transitions can be expressed as

$$W(\theta; I_i \rightarrow I_{i-1}) = 1 + Q_2 A_2^i P_2(\theta) + Q_4 A_4^i P_4(\theta), \quad (3)$$

where Q_2 and Q_4 are geometrical attenuation coefficients which take into account the finite size of the detectors [18], $P_2(\theta)$ and $P_4(\theta)$ are Legendre polynomials and A_2^i and A_4^i are given by [19]

$$A_k^i \equiv A_k[w^{I_i}(M)] = B_k(I_i) R_k(2\ 2\ I_i\ I_{i-1}), \quad (4)$$

$$i = n, \ldots, n_{\max} \text{ and } k = 2, 4$$

with

$$B_k(I_i) = \sum_{M=0}^{M=I_i} w^{I_i}(M)\ \rho_k(I_i, M), \quad (5)$$

where R_k are tabulated coefficients, ρ_k are statistical tensor coefficients, and $w^{I_i}(M)$ are the substate populations for the state with spin I_i. In the present experiments with cylindrical symmetry only the $M = 0$ and $M = \pm 1$ states need to be taken into account; they satisfy the normalization condition

$$w^{I_i}(M = 0) + 2w^{I_i}(M = -1, 1) = 1. \quad (6)$$

In the analysis, the measured angular distributions of all cascade transitions are fitted simultaneously by minimizing

$$\chi^2 = \sum_{n=1}^{n_{\max}} \chi_n^2, \quad (7)$$

where the χ_n^2 are defined by

$$\chi_n^2 = \sum_j \frac{[W^n(\theta_j; I_n \rightarrow I_{n-1}) - W^n_{\text{meas}}(\theta_j; I_n \rightarrow I_{n-1})]^2}{[\delta W^n_{\text{meas}}(\theta_j; I_n \rightarrow I_{n-1})]^2}, \quad (8)$$

W^n_{meas} are the measured γ-ray intensities of the $I_n \rightarrow I_{n-1}$ transitions at angles θ_j, and δW^n_{meas} are the statistical errors.

With values for A_2^i's and A_4^i's from Eq. (4) and an assumed set of $w^{I_n}(0)$ parameters, the angular distributions are fitted to determine the direct excitation parameters. Because the population parameters were at first arbitrarily chosen, the whole calculation is repeated for a range of substate population parameters in order to establish a minimum in the χ^2 surface in the $n_{\max} + 1$ dimensional space. The analysis of the data for run V for instance shows that the 2_1^+ state has a well-defined population parameter at $w^{2_1^+}(0) = 0.92$. If the population parameter is fixed at that value, $\chi^2_{2_1^+}$ exhibits a shallow minimum at $w^{4_1^+}(0) = 0.96$. The final results for the direct excitation probabilities obtained from the analysis of the angular correlations are shown in Table III. The results are insensitive to the particular choice of population parameters $w(M)$ and are in good agreement with excitation probabilities calculated from the statistical tensors obtained with the COULEX code for a "rotational" ^{150}Sm nucleus.

Figures 4, 5, and 6 show the angular distributions obtained from the simultaneous fits of the data from runs IV, V, and VII.

B. Precession analysis

The procedure for extracting $\Delta\theta_i$, the angle of precession of the magnetic moment of the directly excited

TABLE III. Comparison of the direct excitation probabilities P_I extracted from a simultaneous fit of all angular correlations with the excitation probabilities P_I^{Coulex} obtained from the Coulex code. The $P_{\text{g.s.}}^{\text{Coulex}}$ were used to normalize the experimental P_I's.

Run	$P_{\text{g.s.}}^{\text{Coulex}}$	$P_{2_1^+}$	$P_{2_1^+}^{\text{Coulex}}$	$P_{4_1^+}$	$P_{4_1^+}^{\text{Coulex}}$	$P_{6_1^+}$	$P_{6_1^+}^{\text{Coulex}}$
I	0.796		0.196		0.008		0.0001
II	0.308	0.315	0.303	0.385	0.281	-[a]	0.098
IV	0.308	0.339	0.245	0.248	0.316	0.105	0.132
V	0.433	0.456	0.419	0.111	0.133		0.014
VI	0.832		0.163		0.005		0.0001
VII	0.386	0.435	0.468	0.179	0.132		0.013

[a]The $6_1^+ \rightarrow 4_1^+$ transition was too weak in the NaI(Tl) spectra to be analyzed.

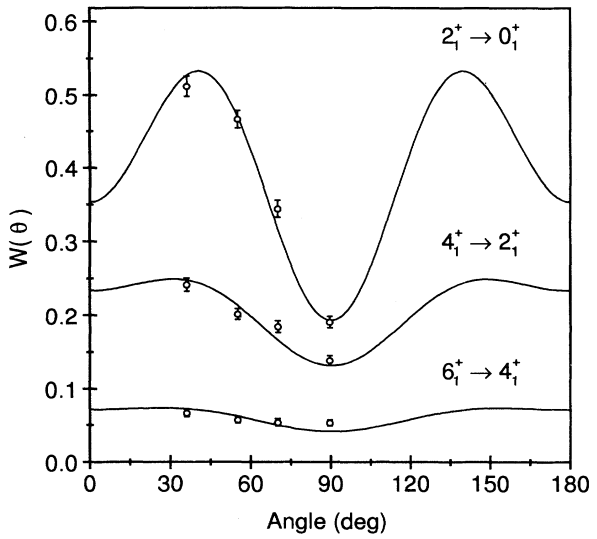

FIG. 4. Simultaneously fitted angular correlations of the $6_1^+ \rightarrow 4_1^+$, $4_1^+ \rightarrow 2_1^+$, and $2_1^+ \rightarrow 0_1^+$ transitions in ^{150}Sm measured in run IV with a 230 MeV ^{58}Ni beam.

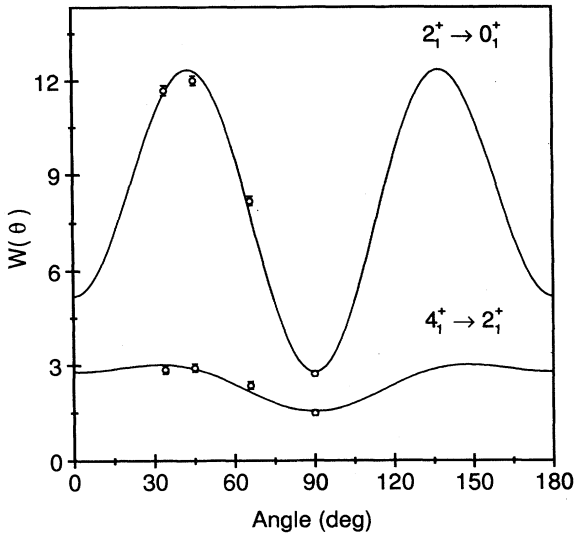

FIG. 6. Simultaneously fitted angular correlation of $4_1^+ \rightarrow 2_1^+$ and $2_1^+ \rightarrow 0_1^+$ transitions in ^{150}Sm measured in run VII with a 115 MeV ^{32}S beam.

i^{th} state from the variation in the counting rates as a function of the magnetic field direction, has been outlined previously [20,15] for cases in which the states are excited by single or multiple Coulomb excitation. If, as is the case in this work, lifetimes of all states of interest are much larger than the transit times of the ions through the ferromagnetic layer, then the nucleus in any given state undergoes a precession in the ferromagnetic foil only when the state is directly populated. The measured effects ϵ can then be written in terms of the relative excitation probabilities P_i and the logarithmic slopes S_i of the angular distributions $W(\theta_0; I_i \rightarrow I_{i-1})$ of radiations deexciting the ith state as

$$\epsilon_n(\theta_0) = \frac{\sum_{i=n}^{n_{\max}} P_i W(\theta_0) S_i \Delta\theta_i}{\sum_{i=n}^{n_{\max}} P_i W(\theta_0)}, \tag{9}$$

where θ_0 is the angle at which the measurements were carried out. P_i and S_i were extracted from the simultaneous fits of the measured angular distributions. The measured effect can be expressed as

$$\epsilon_n(\theta_0) = \frac{\rho^n - 1}{\rho^n + 1}, \tag{10}$$

where $\rho^n = (\rho^n_{14}/\rho^n_{23})^{1/2}$ is determined from the double ratios [11]

$$\rho^n_{kl} = \sqrt{\frac{N_k^{\uparrow n}/N_k^{\downarrow n}}{N_l^{\uparrow n}/N_l^{\downarrow n}}}, \tag{11}$$

where the coefficients $k = 1,2$, $l = 3,4$ represent the four detectors; $N_k^{\uparrow n}$ and $N_k^{\downarrow n}$ are the random- and background-subtracted coincidence counting rates of the photopeak of the transition $I_n \rightarrow I_{n-1}$ in the kth or lth detector with the external field up($\uparrow$) or down($\downarrow$) with respect to the plane of the reaction. Similar "cross ratios," $\rho_c = (\rho_{24}/\rho_{13})^{1/2}$ and ϵ_c, were calculated from the data in order to check for systematic effects that might mask the true precession. In all cases, vanishingly small ϵ_c were obtained.

As evident from the previous section, the errors in the degree of alignment of the 4_1^+ or 6_1^+ states cannot be determined by the fitting procedure because of the insensitivity of the fits to the population parameters. It is important, however, to examine the effect of uncertainties in the population parameters on the precession angles. The population parameter of the 2_1^+ state was

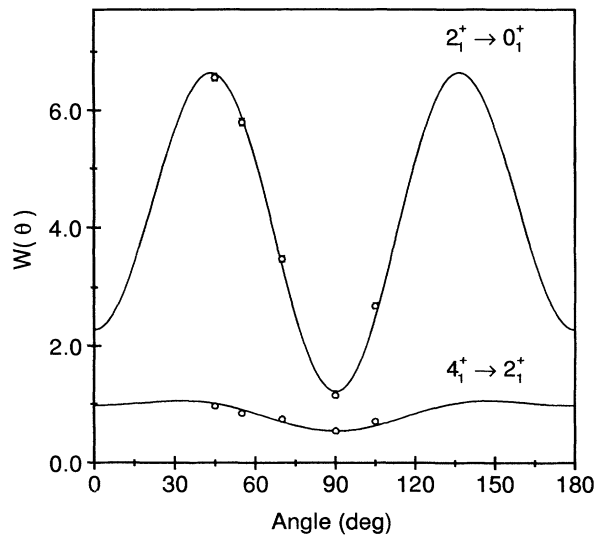

FIG. 5. Simultaneously fitted angular correlation of $4_1^+ \rightarrow 2_1^+$ and $2_1^+ \rightarrow 0_1^+$ transitions in ^{150}Sm measured in run V with a 180 MeV ^{58}Ni beam.

TABLE IV. Summary of the measured asymmetry ratios ϵ, the calculated precession angles $\Delta\theta$ (in mrad), and the magnetic moment ratios of the excited states of the ^{150}Sm nuclei.

	Run I	Run II	Run III	Run IV	Run V	Run VII	Ref. [15]
ϵ_{2+}	0.065(3)	0.043(4)	0.056(4)	0.079(3)	0.070(2)	0.040(2)	0.063(1)[b]
ϵ_{4+}		0.041(8)	0.049(6)	0.062(5)	0.045(5)	0.024(5)	0.030(2)[b]
ϵ_{6+}		-[a]	-[a]	0.039(11)			0.026(4)[b]
$\Delta\theta_{2+}$	-22.7(1.0)	-22.5(4.1)	-26.7(3.5)	-38.0(3.6)	-24.9(8)	-16.2(1.1)	-34.2(2.7)
$\Delta\theta_{4+}$		-40.9(7.7)	-46.76(6.2)	-64.1(7.6)	-38.7(4.0)	-22.3(5.0)	-29.7(2.5)
$\Delta\theta_{6+}$		-[a]	-[a]	-43.4(12.2)			-32.0(6.0)
$\frac{g_{4_1^+}}{g_{2_1^+}}$		1.82(47)[c]	1.75(33)[c,d]	1.68(26)	1.56(17)	1.37(32)	0.87(10)
$\frac{g_{6_1^+}}{g_{2_1^+}}$		-[a]	-[a]	1.14(34)			0.94(19)

[a]The $6_1^+ \rightarrow 4_1^+$ transition was too weak in the NaI(Tl) detectors to be analyzed and ϵ and $\Delta\theta$ were obtained as though the 6_1^+ state had not been excited at all.
[b]Private communication from Stuchbery.
[c]This ratio assumes the 6_1^+ state has not been excited.
[d]Since the conditions of runs III and IV were identical except for the different detectors, the results of run III could be reanalyzed assuming the effect $\epsilon(6_1^+)$ to be the same as that observed in run IV, namely 0.039(11). The resulting ratio $g(4_1^+)/g(2_1^+) = 1.85(49)$ is well within the statistical error obtained by neglecting the contribution from the 6_1^+ state. If $\epsilon(6_1^+)$ were to be varied by 20%, the ratio would only change by 5%.

kept fixed at the well-defined minimum, while the population parameters of the 4_1^+ and 6_1^+ states were changed independently over a fairly wide range. The changes in the resulting precessions were smaller than the statistical errors.

The g factors may be obtained from the observed precession through the following expression:

$$\Delta\theta = -g \frac{\mu_N}{\hbar} \int_0^{t_m} B(v,Z) \exp(-t/\tau) dt \,, \qquad (12)$$

where μ_N is the nuclear magneton, $B(v,Z)$ is the transient field, t_m is the transit time through the ferromagnetic foil, and τ is the meanlife of the state. Since t_m is short compared to the mean lifetimes of the states, the ratios of g factors are equal to ratios of the measured precession angles $\Delta\theta$ and are independent of a precise knowledge of the transient field.

The experimentally determined precession effects ϵ, the precession angles $\Delta\theta$, and g-factor ratios for each measurement in this study are displayed in Table IV, and the ratios $g(4_1^+)/g(2_1^+)$ are plotted in Fig. 7.

IV. DISCUSSION

The ratios of g factors obtained in the various runs are in good agreement with each other. However, they disagree with the theoretical prediction for magnetic moments within a collective band, $g(I+2)/g(I) \approx 1$, and are significantly larger than the ratios obtained in the experiment of Ref. [15]. As previously discussed, the ratio of g factors should be independent of the specific experimental conditions. However, in this case the 2_1^+ and 4_1^+ states have very different lifetimes. If some of the recoiling Sm ions were to stop in the ferromagnet, the long-lived 2_1^+ state would precess in the static hyperfine field, while the short-lived 4_1^+ state would not. Unfortunately, the static fields at Sm ions embedded in iron or gadolinium hosts are not well known [21]. The static hyperfine field at Sm ions in iron at 300 K varies from +0.140(16) to +0.22 kT, while the value of the static field at Sm ions in gadolinium at 1.5 K has been quoted as lying between −0.0295(30) and (−)0.3648(21) kT. With these rather large static fields, even if only a small number of ions

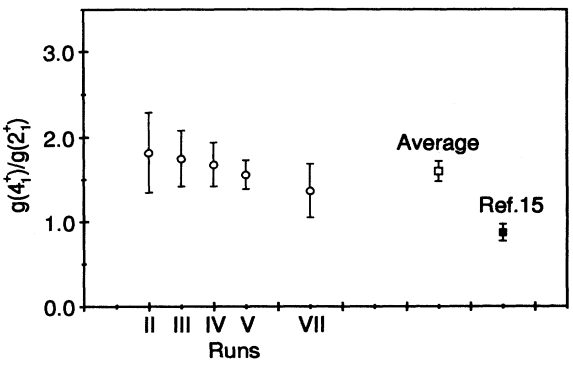

FIG. 7. g-factor ratios $g(4_1^+)/g(2_1^+)$ in ^{150}Sm as measured in different runs (open circles). The weighted average of the $g(4_1^+)/g(2_1^+)$ ratios for runs II–V and VII is indicated by an open square and the ratio measured in Ref. [15] by the solid square.

stop in the ferromagnetic host, their contribution to the measured precession can be appreciable. The total observed precession will be increased for the positive static field in iron and decreased for the negative static field in gadolinium.

The total measured precession can be written as

$$\Delta\theta^{\text{meas}} = \Delta\theta^{\text{TF}} + x\,\Delta\theta^{\text{static}}, \tag{13}$$

where $0 \leq x \leq 1$ is the fraction of ions that stop in the ferromagnet, $\Delta\theta^{\text{TF}}$ is the precession resulting from the transient field interaction, and the contribution due to precession in the static field is given by

$$\Delta\theta^{\text{static}} = -g\,\frac{\mu_N}{\hbar}\,B_{\text{static}}\tau, \tag{14}$$

where τ and g are, respectively, the mean lifetime and g factor of the state of interest. Thus, the ratio of the g factors becomes

$$\frac{g_{4_1^+}}{g_{2_1^+}} \simeq \frac{\Delta\theta^{\text{meas}}_{4_1^+}}{\Delta\theta^{\text{meas}}_{2_1^+}} \simeq \frac{\Delta\theta^{\text{TF}}_{4_1^+}}{\Delta\theta^{\text{TF}}_{2_1^+} + x\,\Delta\theta^{\text{static}}_{2_1^+}}\,. \tag{15}$$

An experimental test of possible static field contributions was carried out in which the energy of the ^{58}Ni beam was decreased to 120 MeV using the target of runs III–V. A strong angular correlation with a logarithmic slope $S = -3.18(29)$ was measured for the 2_1^+ state and a precession with opposite sign to that observed in the higher-energy experiments was observed (Table V), indicating that the precession in the static field does indeed dominate the precession in the transient field. From this measurement, the known value of $g(2_1^+)$, and an assumed static field $B = 0.3648$ kT, the fraction of stopping ions was determined to be $x = 12\%$.

This result was corroborated by calculating the fraction of stopped ions via a Monte Carlo simulation of the slowing down process using Ziegler's TRIM-91 code [22]. Figure 8(a) shows the range distribution of ions throughout the target, with the dashed line representing the interface between the ferromagnet and the backing. The result of this calculation yields $x = 16\%$ in qualitative agreement with experimental results. However, the fraction of stopped ions is a very sensitive function of the target thickness, as shown in Fig. 8(b). The Monte Carlo calculation was then carried out for all target-beam combinations used in the present study. In all cases the percentage of stopped ions was found to be negligible.

TABLE V. Measured asymmetry ratios ϵ and calculated precession angles $\Delta\theta$ (in mrad) for 120 MeV ^{58}Ni (run VI). The positive value for the angular precession of the 2_1^+ state is indicative of a large precession in the static field at Sm in gadolinium.

	2_1^+	4_1^+
ϵ	-0.022(5)	0.042(37)
$\Delta\theta$	6.9(1.7)[a]	-36.5(32.2)[a]

[a]The feeding of the 2_1^+ state from higher states is negligible (see Table III). The precession angles were calculated with the logarithmic slope of the pure $2_1^+ \rightarrow 0_1^+$ [$S = -3.18(29)$] and $4_1^+ \rightarrow 2_1^+$ ($S = -1.15$) transitions.

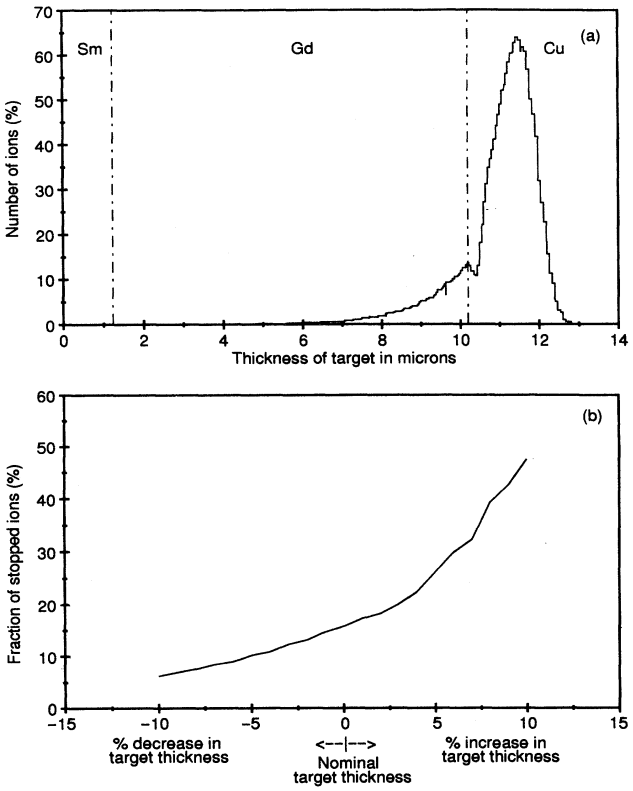

FIG. 8. (a) Monte Carlo simulated range distribution of ^{150}Sm recoils, assuming the target and beam arrangement used in run VI, (b) dependence of the fraction of ions stopped in the ferromagnet on the Sm and gadolinium target thickness.

In Ref. [15] a possible contribution from the static field was not taken into account. In order to check the discrepancy in the g-factor ratio between Ref. [15] and the present work, Monte Carlo calculations were carried out for the data of Ref. [15]. The calculation indicates that 1.6(0.9)% of the ions might stop in the iron layer. The error quoted reflects a 3% uncertainty in the target thickness. This result would add 3.0(1.7) to 4.7(2.7) mrad to the transient field precession, depending on the actual value of the static field at Sm ions in iron. However, the inclusion of the static field contribution is not large enough to explain the discrepancy in the g-factor ratios.

The ratio of g factors for runs II–V and VII are shown in Fig. 7. All results are consistent with each other even though they were obtained under radically different experimental conditions, and yield an average $g(4_1^+)/g(2_1^+) = 1.60(12)$. The resulting $g(4_1^+)/g(2_1^+)$ is unexpectedly large. This large ratio cannot be explained through purely collective excitations or through IBA models with either a restricted *sd*-boson or an extended *sdg*-boson basis [23]; it must involve decoupling single particles yield-

ing a higher magnetic moment for the 4_1^+ state. In the most naive shell model, one could construct the low-lying states with protons in $d_{5/2}$ and neutrons in $h_{9/2}$ shells for which $g = 1.13$ [24]. Thus even a small admixture of such configurations could indeed result in magnetic moments that deviate from the predictions presented above. A more specific explanation will have to wait for new single-particle calculations, an examination of the structure of this vibrational nucleus within the framework of the IBA model or more detailed calculations of the effects of deformation on pairing gaps and alignments.

A future measurement of the magnetic moments of the low-lying states of ^{152}Gd could also help elucidate the structure of the $N = 88$ isotones in terms of particle-collective core interactions, IBA models, or the BCS picture with deformation and spin dependence on angular momentum.

V. CONCLUSIONS

The magnetic moment ratios $g(4_1^+)/g(2_1^+)$ and $g(6_1^+)/g(2_1^+)$ in ^{150}Sm have been measured by the transient field technique in a variety of experiments involving different targets mounted on different magnetic materials, different beams at different energies, and different detectors. While individual moments may be very sensitive to the details of the transient field velocity dependence and target inhomogeneities, ratios of moments ought to be free from such systematic errors. The results are consistent with each other from run to run but yield ratios that are too large compared with previous experiments as well as with current theoretical predictions. Future experiments with increased accuracy as well as similar measurements in ^{152}Gd may yield an explanation of these discrepancies.

ACKNOWLEDGMENTS

We wish to thank A. Lipski and R. Klein for their assistance in target preparation. We also acknowledge the help and support of the students and technical staff of the Wright Nuclear Structure Laboratory. This work was supported in part by the National Science Foundation.

[1] A. Bohr and B. R. Mottelson, *Nuclear Structure* (Benjamin, Reading, MA, 1975), Vol. II, p. 54.
[2] A. Wolf, D. D. Warner, and N. Benczer-Koller, Phys. Lett. **158B**, 7 (1985).
[3] N. Benczer-Koller, D. J. Ballon, and A. Pakou, Hyperfine Interact **33**, 37 (1987).
[4] A. Wolf, R. F. Casten, and D. D. Warner, Phys. Lett. B **190**, 19 (1987).
[5] N. Benczer-Koller and G. Kumbartzki, in *Proceedings of the International Conference on Understanding the Variety of Nuclear Excitations*, Ischia, 1990, edited by A. Covello (World Scientific Publishing Company, Singapore, 1991), p. 619. A review of magnetic moment measurements of high-spin states is presented in this paper accompanied by extensive references.
[6] F. Brandolini, P. Pavan, D. Bazzacco, C. Rossi-Alvarez, R. V. Ribas, M. de Poli, and A. M. Haque, Phys. Rev. C **45**, 1549 (1992).
[7] S. Frauendorf, Phys. Lett. **100B**, 219 (1981); Y. S. Chen and S. Frauendorf, Nucl. Phys. **A393**, 135 (1983).
[8] A. Ansari, E. Wüst, and K. Mühlhans, Nucl. Phys. **A415**, 215 (1984).
[9] R. Bengtsson and S. Åberg, Phys. Lett. B **172**, 277 (1986).
[10] H. Hübel, S. Heppner, U. Birkental, G. Baldsiefen, A. P. Byrne, M. Schmitz, M. Bentley, P. Fallon, P. D. Forsyth, D. Howe, J. R. Roberts, H. Kluge, G. Goldring, A. Dewald, G. Siems, and E. Lubkiewicz, Prog. Part. Nucl. Phys. **28**, 295 (1992).
[11] N. K. B. Shu, D. Melnik, J. M. Brennan, W. Semmler, and N. Benczer-Koller, Phys. Rev. C **21**, 1828 (1980).
[12] N. Benczer-Koller, M. Hass, and J. Sak, Annu. Rev. Nucl. Sci. **30**, 53 (1980).
[13] I. Ben-Zvi, P. Gilad, M. B. Goldberg, G. Goldring, K. H. Speidel, and A. Sprinzak, Nucl. Phys. **A151**, 401 (1970).
[14] H. W. Kugel, R. R. Borchers, and R. Kalish, Nucl. Phys. **A186**, 513 (1972).
[15] A. P. Byrne, A. E. Stuchbery, H. H. Bolotin, C. E. Doran, and G. J. Lampard, Nucl. Phys. **A466**, 419 (1987).
[16] Preliminary results were reported by T. Vass, G. Kumbartzki, C. Whitaker, N. Benczer-Koller, and R. Tanczyn, Bull. Am. Phys. Soc. **36**, 2149 (1991).
[17] A. Piqué, J. M. Brennan, R. Darling, R. Tanczyn, D. Ballon, and N. Benczer-Koller, Nucl. Instrum. Methods A **279**, 579 (1989).
[18] K. S. Krane, Nucl. Instrum. Methods **98**, 205 (1972).
[19] H. L. Rose and D. M. Brink, Rev. Mod. Phys. **39**, 306 (1967).
[20] A. E. Stuchbery, I. Morrison, L. D. Wood, R. A. Bark, H. Yamada, and H. H. Bolotin, Nucl. Phys. **A435**, 635 (1985); A. E. Stuchbery, C. G. Ryan, and H. H. Bolotin, S. H. Sie, Phys. Rev. C **4**, 1618 (1981).
[21] G. N. Rao, Hyperfine Interact **7**, 141 (1979).
[22] J. F. Ziegler, TRIM, "The Transport of Ions in Matter," 1992, PC program provided by the author.
[23] I. Morrison, Phys. Lett. B **175**, 1 (1986).
[24] L. Zamick, private communication.